DOI: 10.1017/S1431927603444802
Microsc Microanal 9(Suppl 2), 2003

Information Localization in the Electron Microscope

A. R. Lupini, S. J. Pennycook, A. Y. Borisevich.

Condensed Matter Sciences Division, Oak Ridge National Laboratory, Oak Ridge, TN 37831

Historically, the resolution achievable in an electron microscope has been limited by the unavoidable aberrations of the lenses used to form the image [1]. However recently, aberration correctors have been shown to be able to improve both the ultimate resolution attainable, and the current available to form the image at any given resolution [2]. The resolution in aberration corrected instruments will soon approach the quantum mechanical limits, and we investigate how these limits depend on the imaging mode used.

The scanning transmission electron microscope (STEM) offers several advantages over the conventional transmission electron microscope. These advantages include reduced sensitivity to chromatic effects, opportunities for single atom visualization and potentially higher resolution in the Z-contrast imaging mode [3]. The STEM can also provide simultaneous bright field and dark field images. Fig. 1 shows aberration corrected images of γ-alumina doped with lanthanum. This system generates considerable industrial interest as a support material for catalysts [4]. Single lanthanum atoms are visible in the high angle annular dark field image (HAADF) image, but not in the bright field image (which by reciprocity is equivalent to the conventional TEM image). The differences between the bright field and HAADF image show how the localization of the image depends on the detector as well as the illumination system. Since these two images were recorded simultaneously, they both have the same exit wavefunction intensity. This suggests that in order to consider the localization of the information in the image, it could be misleading to simply consider the intensity distribution in the exit wave function.

We can understand how these differences arise by instead considering the distribution of electron intensity as seen from the detector. In real space, the exit wavefunction for a probe at position $\mathbf{R}_0$ is $\psi(\mathbf{R},\mathbf{R}_0)$. The observable is the intensity which is incident on the detector. Because the detector cannot measure the phase, we use Parseval's theorem to write the observable intensity for a particular detector, as:

$$I(\mathbf{R}_0) = \int \left| \psi(\mathbf{R},\mathbf{R}_0) \otimes d(\mathbf{R}) \right|^2 d\mathbf{R} \qquad (1)$$

Where d(**R**) is the Fourier transform of the detector function, D(**K**), which is unity over the range of scattering angles accepted by the detector and zero elsewhere.

It has been shown that it is not simply the intensity in the exit wavefunction that is recorded, but rather this wavefunction must be convolved with the detector function first. The intensity from equation (1) is plotted out in fig. 2 for several different detector functions. Fig. 2. shows that the area of the sample contributing significantly to the image at each probe position decreases with increasing detector size. This result demonstrates the importance of including the detector in all image simulations, and shows how it is possible for images recorded simultaneously in the STEM to have such different appearance and sensitivity to single dopant atoms.

References

[1] O. Scherzer, *J. Appl. Phys*. 20 (1949) 20.
[2] P. E. Batson et al., *Nature* 418 (2002) 617.
[3] P. D. Nellist et al, *Ultramicroscopy* 78 (1999) 111.
[4] A. Y. Borisevich et al., *These proceedings* (2003).

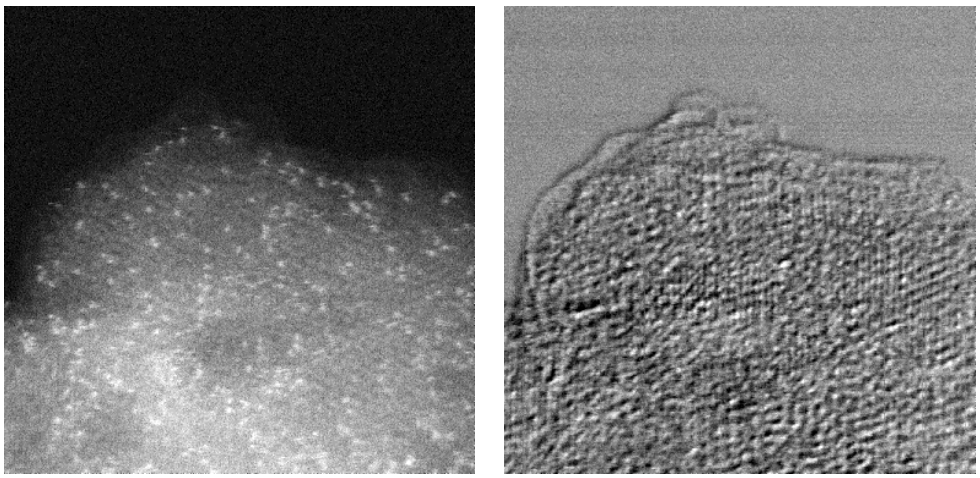

Fig. 1. HAADF (left) and BF (right) (equivalent to coherent TEM) images of single La atoms in alumina, recorded simultaneously in the 300 kV STEM at ORNL.

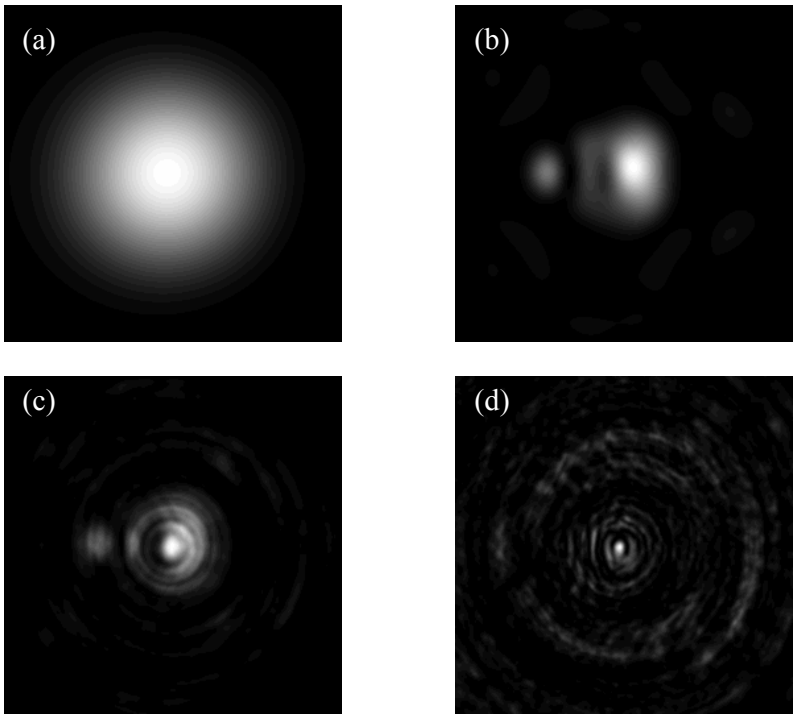

Fig 2. Multislice simulations of the spatial distribution of intensity for a probe located over one column in Si [110] as seen by various detectors. (a) 0-3 mrad, (b) 0-15 mrad, (c) 15-200 mrad. (d) 30-200 mrad. For a probe with Cs=0.5 mm, defocus=-43 nm, aperture 13.3 mrad, with specimen thickness 76.8 Å, 10 phonons at 300 K.

https://doi.org/10.1017/S1431927603444802 Published online by Cambridge University Press